

See discussions, stats, and author profiles for this publication at: <https://www.researchgate.net/publication/227394952>

Phase diagrams of binary mixtures of liquid crystals and rodlike polymers in the presence of an external field

ARTICLE *in* THE JOURNAL OF CHEMICAL PHYSICS · JUNE 2012

Impact Factor: 2.95 · DOI: 10.1063/1.4728337 · Source: PubMed

CITATIONS

2

READS

14

2 AUTHORS, INCLUDING:



Akihiko Matsuyama

Kyushu Institute of Technology

72 PUBLICATIONS 796 CITATIONS

SEE PROFILE

Phase diagrams of binary mixtures of liquid crystals and rodlike polymers in the presence of an external field

Akihiko Matsuyama and Tomomi Ueda

Citation: *J. Chem. Phys.* **136**, 224904 (2012); doi: 10.1063/1.4728337

View online: <http://dx.doi.org/10.1063/1.4728337>

View Table of Contents: <http://jcp.aip.org/resource/1/JCPSA6/v136/i22>

Published by the [American Institute of Physics](#).

Additional information on J. Chem. Phys.


Journal Homepage: <http://jcp.aip.org/>

Journal Information: http://jcp.aip.org/about/about_the_journal

Top downloads: http://jcp.aip.org/features/most_downloaded

Information for Authors: <http://jcp.aip.org/authors>

ADVERTISEMENT



AIPAdvances

Special Topic Section:
PHYSICS OF CANCER

Why cancer? Why physics? [View Articles Now](#)

Phase diagrams of binary mixtures of liquid crystals and rodlike polymers in the presence of an external field

Akihiko Matsuyama^{a)} and Tomomi Ueda

Department of Bioscience and Bioinformatics, Faculty of Computer Science and Systems Engineering,
Kyushu Institute of Technology, Kawazu 680-4, Iizuka, Fukuoka 820-8502, Japan

(Received 26 April 2012; accepted 24 May 2012; published online 12 June 2012)

We theoretically study phase separations in mixtures of a low molecular-weight-liquid crystalline molecule (LC) and a rigid-rodlike polymer (rod) under an external field, such as magnetic or electric fields. By taking into account two orientational order parameters of the rod and the LC, we define four nematic phases (N_0, N_1, N_2, N_3) on the temperature-concentration plane. Depending on the sign of the dielectric anisotropy $\Delta\epsilon_i$ of the rod ($i = 1$) and LC ($i = 2$), we examine the phase behavior of rod/LC mixtures in the case of $\Delta\epsilon_1 > 0, \Delta\epsilon_2 > 0$ (a), $\Delta\epsilon_1 < 0, \Delta\epsilon_2 > 0$ (b), $\Delta\epsilon_1 > 0, \Delta\epsilon_2 < 0$ (c), and $\Delta\epsilon_1 < 0, \Delta\epsilon_2 < 0$ (d). We predict a variety of phase separations induced by an external field.
© 2012 American Institute of Physics. [<http://dx.doi.org/10.1063/1.4728337>]

I. INTRODUCTION

Alignment of rigid-rodlike polymers in liquid crystalline solvents has been the current topic in physics and material science.^{1–14} Recently, we have presented a mean field theory to describe phase separations in binary mixtures of a low-molecular weight liquid crystal (LC) and a long rigid-rodlike polymer (rod),¹⁵ including carbon nanotube,^{16–18} Kevlar: a rigid-rodlike polymer of poly(p-phenylene terephthalamide),¹⁹ tobacco mosaic virus,²⁰ and liquid crystalline polymers. By taking into account two orientational order parameters of the rod and the LC, we have predicted three uniaxial nematic phases (N_0, N_1, N_2) on the temperature-concentration plane, depending on the attractive or repulsive interactions between the rod and the LC. Biaxial nematic phases in rod/LC mixtures have also been predicted.²¹ It is well known that such rods and LCs can be reoriented in the presence of an external field such as electric or magnetic fields.^{22–27}

In this paper, we consider the phase behavior of rod/LC mixtures in the presence of the external fields. When the external magnetic or electric field applies to the system (parallel to z axis), we can expect four types of uniaxial nematic phases. Figure 1 schematically shows the four uniaxial nematic phases, defined by using the orientational order parameter (S_1) of the rod and that (S_2) of the LC. In this paper, we consider uniaxial nematic phases. The nematic N_0 phase shows the rods and the LCs are parallel to the field: $S_1 > 0$ and $S_2 > 0$. The nematic N_1 phase is defined as that the rods are perpendicular to the external field and the LCs are parallel to the field: $S_1 < 0$ and $S_2 > 0$. In this phase, the rods are randomly distributed within the perpendicular plane to the external field (note that there is no positional order for rods along z axis). The nematic N_2 phase is defined as that the rods are parallel to the external field and the LCs are perpendicular to the field: $S_1 > 0$ and $S_2 < 0$. The LCs are randomly distributed within the perpendicular plane to the external field.

The nematic N_3 phase is defined as that the rods and LCs are randomly distributed within the perpendicular plane to the external field: $S_1 < 0$ and $S_2 < 0$. These nematic phases can be formed by depending on the positive or negative dielectric (or diamagnetic) anisotropy $\Delta\epsilon_i$ of the rod ($i = 1$) and LC ($i = 2$). For example, when the dielectric anisotropy $\Delta\epsilon_1$ of the rods is positive and the $\Delta\epsilon_2$ of LCs is negative, we can expect the N_2 phase in the presence of a strong electric field. Moreover, in a weak external field, the interaction between the rod and LC can prevail the system. We then expect that the phase behavior of the mixtures can be changed by the coupling between the dielectric anisotropy and the strength of the external field.

In order to predict theoretically the phase diagrams of the rod/LC mixtures in the presence of an external field, we extend the previous model¹⁵ to this system by taking into account the interaction between an external field and each component. Depending on the interaction between the rod and LC and the strength of the external field, we find a variety of phase separations.

II. THEORY

We here briefly introduce the free energy of mixtures of a rod and a LC.¹⁵ We consider a binary mixture of N_1 rigid-rodlike polymers (rods) of length L_1 and diameter D_1 and N_2 low-molecular weight LC molecules of length L_2 and diameter D_2 : $L_1 \gg L_2$. The volume of the rod and that of the LC are given by $v_1 = (\pi/4)D_1^2L_1$ and $v_2 = (\pi/4)D_2^2L_2$, respectively, where $V = v_1N_1 + v_2N_2$. Let $\phi_1 = v_1N_1/V$ and $\phi_2 = v_2N_2/V$ be the volume fraction of the rod and LC, respectively. Using the axial ratio $n_1 \equiv L_1/D_1$ of the rod and $n_2 \equiv L_2/D_2$ of the LC, the volume per particle is given by $v_1 = a^3n_1$ and $v_2 = a^3n_2$, where we assume $D \equiv (D_1 = D_2)$ and define $a^3 \equiv (\pi/4)D^3$.

The free energy F of the rod/LC mixture is given by¹⁵

$$F = F_{\text{mix}} + F_{\text{nem}} + F_{\text{ext}}. \quad (1)$$

^{a)}URL: <http://iona.bio.kyutech.ac.jp/~aki/>.

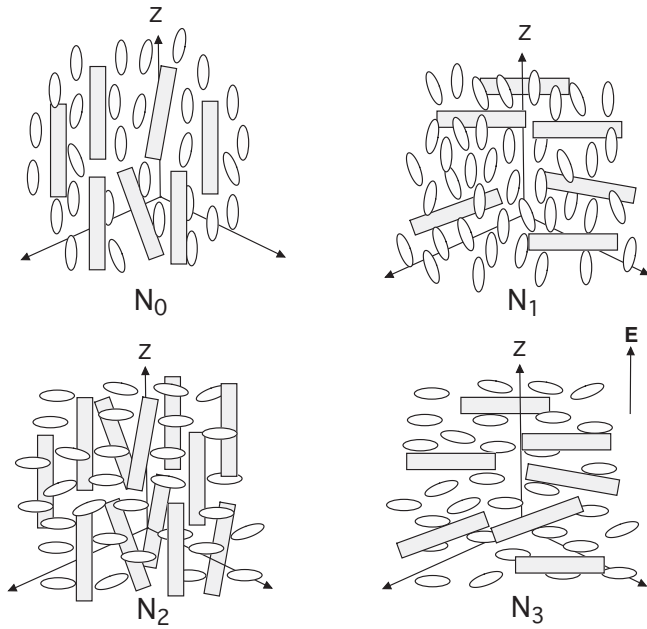


FIG. 1. Schematically illustrated four possible uniaxial nematic phases in the presence of the external field, parallel to z axis. The nematic phases are defined by using the orientational order parameter S_1 of the rod and that S_2 of the LC: nematic N_0 phase with $S_1 > 0$ and $S_2 > 0$, nematic N_1 phase with $S_1 < 0$ and $S_2 > 0$, nematic N_2 phase with $S_1 > 0$ and $S_2 < 0$, and N_3 phase with $S_1 < 0$ and $S_2 < 0$.

The first term shows the free energy for mixing of rods and LCs in the isotropic phase

$$a^3 \beta F_{mix}/V = \frac{\phi_1}{n_1} \ln \phi_1 + \frac{\phi_2}{n_2} \ln \phi_2 + \chi \phi_2 \phi_1, \quad (2)$$

where $\beta \equiv 1/k_B T$; T is the absolute temperature, k_B is the Boltzmann constant. The first and the second terms correspond to the entropy of isotropic mixing for rods and LCs, respectively, and the last term shows the Flory-Huggins interaction parameter χ ($\equiv U_0/k_B T$) between a rod and a LC, where U_0 is the interaction energy between the rod and the LC in an isotropic state.²⁸ A positive χ denotes that the rod-LC contacts are less favored compared with the rod-rod and LC-LC contacts.

The second term in Eq. (1) shows the free energy for nematic ordering²⁹

$$a^3 \beta F_{nem}/V = \sum_{i=1,2} \frac{\phi_i}{n_i} \int f_i(\theta) \ln 4\pi f_i(\theta) d\Omega - \frac{1}{2}(\nu_1 + 5/4)\phi_1^2 S_1^2 - \frac{1}{2}\nu_2\phi_2^2 S_2^2 - \nu_{12}\phi_1\phi_2 S_1 S_2, \quad (3)$$

where $d\Omega = 2\pi \sin \theta d\theta$, ν_1 ($\equiv U_1/k_B T > 0$) is the anisotropic attractive (Maier-Saupe) interaction parameter between rods,^{30,31} and ν_2 ($\equiv U_2/k_B T > 0$) is the anisotropic attractive interaction between LCs. The anisotropic interaction ν_{12} ($\equiv U_{12}/k_B T$) between a LC and a rod can be positive or negative value. The term ν_1 and $5/4$ correspond to the attractive and excluded volume interactions between rods, respectively.^{15,32} We here assume that the excluded volume

interaction between LCs can be negligible because the length of LC is short.

The orientational order parameter S_i ($i = 1, 2$) of a nematic phase is given by²²

$$S_i = \int P_2(\cos \theta) f_i(\theta) d\Omega, \quad (4)$$

where $f_i(\theta)$ is the distribution function of the particle i ($i = 1, 2$) and $P_2(\cos \theta) \equiv 3(\cos^2 \theta - 1/3)/2$.

When $\nu_{12} > 0$ in Eq. (3), LCs prefer along align parallel to rods: $S_1 > 0$ and $S_2 > 0$, to be lower than the nematic free energy. This corresponds to the N_0 and N_3 phases. On the other hand, when $\nu_{12} < 0$, LCs prefer along align perpendicular to rods to be lower than the nematic free energy. This corresponds to either N_1 or N_2 phase.

The last term in Eq. (1) shows the free energy change due to an external field such as electric or magnetic fields. Let $\Delta\epsilon_1 \equiv \epsilon_{1,\parallel} - \epsilon_{1,\perp}$ be a dielectric (or diamagnetic) anisotropy of the rod and $\Delta\epsilon_2 \equiv \epsilon_{2,\parallel} - \epsilon_{2,\perp}$ be a dielectric anisotropy of the LC. When the external electric field \mathbf{E} is applied to the system, the free energy is given by^{22,33,34}

$$\begin{aligned} a^3 \beta F_{ext}/N_t &= -\phi_1 \beta \Delta\epsilon_1 \int (\mathbf{n} \cdot \mathbf{E})^2 f_1(\theta) d\Omega \\ &\quad - \phi_2 \beta \Delta\epsilon_2 \int (\mathbf{l} \cdot \mathbf{E})^2 f_2(\theta) d\Omega \\ &= -\phi_1 \beta \Delta\epsilon_1 E^2 \int \cos^2 \theta f_1(\theta) d\Omega \\ &\quad - \phi_2 \beta \Delta\epsilon_2 E^2 \int \cos^2 \theta f_2(\theta) d\Omega \\ &= -\frac{1}{3}[\phi_1 h_1 (1 + 2S_1) + \phi_2 h_2 (1 + 2S_2)], \end{aligned} \quad (5)$$

where \mathbf{n} and \mathbf{l} are the unit orientation vector of the rod and that of the LC, respectively. We here define the dimensionless external field parameters: $h_1 \equiv \Delta\epsilon_1 \beta E^2$ and $h_2 \equiv \Delta\epsilon_2 \beta E^2$. Depending on the strength of the external field and the positive or negative dielectric anisotropy of the two components, we have four uniaxial nematic phases.

In a thermal equilibrium state, the distribution function $f_1(\theta)$ and $f_2(\theta)$ are determined by minimizing the free energy (1) with respect to these functions: $(\delta F/\delta f_1(\theta))_{\{f_2(\theta)\}} = 0$ and $(\delta F/\delta f_2(\theta))_{\{f_1(\theta)\}} = 0$. We then obtain

$$f_i(\theta) = \frac{1}{4\pi I_0[\Gamma_1]} \exp[\Gamma_1 P_2(\cos \theta)], \quad (6)$$

where

$$\Gamma_1 \equiv n_1 \left[(\nu_1 + 5/4)\phi_1 S_1 + \nu_{12}\phi_2 S_2 + \frac{2}{3}h_1 \right], \quad (7)$$

and the function $I_0[\Gamma_1]$ is defined by

$$I_m[x] \equiv \int_0^1 [P_2(\cos \theta)]^m \exp[x P_2(\cos \theta)] d(\cos \theta), \quad (8)$$

$m = 0, 1, 2$. Substituting Eq. (6) into Eq. (4), we obtain the self-consistency equation for the orientational order

parameter S_1

$$S_1 = I_1[\Gamma_1]/I_0[\Gamma_1]. \quad (9)$$

Similarly, we obtain

$$f_2(\theta) = \frac{1}{4\pi I_0[\Gamma_2]} \exp[\Gamma_2 P_2(\cos \theta)], \quad (10)$$

where we define

$$\Gamma_2 \equiv n_2 \left[v_2 \phi_2 S_2 + v_{12} \phi_1 S_1 + \frac{2}{3} h_2 \right]. \quad (11)$$

Substituting Eq. (10) into Eq. (4), we obtain the self-consistency equation for the orientational order parameter S_1

$$S_2 = I_1[\Gamma_2]/I_0[\Gamma_2]. \quad (12)$$

By numerically solving the coupled equations (9) and (12), we can obtain the values of the nematic order parameters as a function of temperature and concentration.

Substituting Eqs. (6) and (10) into Eq. (3), the free energy F_{nem} of the nematic ordering is given by

$$\begin{aligned} a^3 \beta F_{nem}/V = & \frac{1}{2} (v_1 + 5/4) \phi_1^2 S_1^2 \\ & + \frac{1}{2} v_2 \phi_2^2 S_2^2 + v_{12} \phi_1 \phi_2 S_1 S_2 \\ & - \frac{\phi_1}{n_1} \ln I_0[\Gamma_1] - \frac{\phi_2}{n_2} \ln I_0[\Gamma_2]. \end{aligned} \quad (13)$$

Then the total free energy (1) is given by the sum of Eqs. (2), (5), and (13).

When $\phi_1 = 0$, or pure LCs, the nematic-isotropic phase transitions (NIT) take place at^{22,32}

$$n_2 v_2 = n_2 U_2 / (k_B T_{NI}^\circ) = 4.55, \quad (14)$$

where T_{NI}° shows the NIT temperature of a pure liquid crystal. We here define the reduced temperature

$$\tau \equiv T/T_{NI}^\circ = 4.55/(n_2 v_2). \quad (15)$$

Using the reduced temperature τ , the interaction parameter is given by $v_2 = 4.55/(n_2 \tau)$. The value of n_2 is on the order of one and then the parameter v_2 remains finite values. We here define the anisotropic attractive interaction parameter between LCs

$$\alpha = v_2/\chi, \quad (16)$$

where we take that LCs are good solvents for rods: $\chi \ll 1$. When $\chi = 0$ in a theta solvent, we can remove the parameter α from numerical calculations. The nematic parameter α means that the ratio between the nematic interaction v_2 between LCs and the unfavorable interaction χ between LC and rod in an isotropic phase. On decreasing the value of α , the unfavorable interaction becomes dominant in the free energy.³⁵ The anisotropic attractive interaction parameter between rods is defined as

$$c_1 = v_1/v_2, \quad (17)$$

and we also define

$$c_{12} = v_{12}/v_2, \quad (18)$$

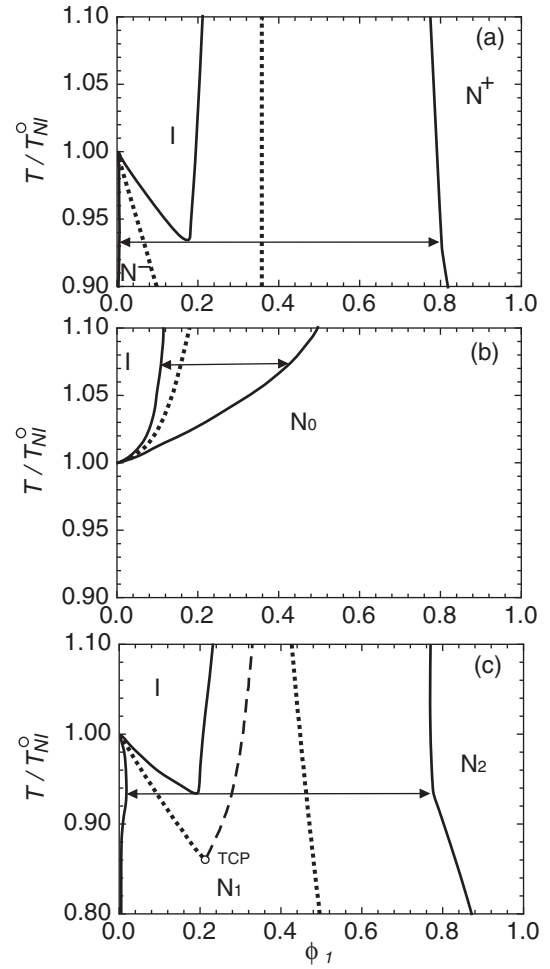


FIG. 2. Typical phase diagrams for $c_{12} = 0$ (a), $c_{12} = 0.5$ (b), and $c_{12} = -0.3$ (c) without the external field: $h_1 = h_2 = 0$.

for the anisotropic interaction parameter between a rod and a LC. The parameters c_1 and c_{12} are on the order of one for dispersion forces. The value of c_{12} becomes important in the phase behavior. The parallel or perpendicular alignments in rod/LC mixtures can be modified by wrapping polymers or surfactants on rod's surface.^{36,37} Hence, it can control the balance between the attractive van der Waals interaction and excluded volume between a LC and a rod. These modifying can control the interaction parameter c_{12} in our model.

III. RESULTS

In this section, we show phase diagrams calculated from the free energy. The coexistence (binodal) curve can be obtained by solving the chemical potential balances between two separated phases and can also be derived by a double tangent method where the equilibrium volume fractions fall on the same tangent line to the free energy curve.¹⁵ In order to calculate phase diagrams, we set $n_1 = 10$, $n_2 = 1$, $\alpha = 10$, and $c_1 = 0$ in the following.

A. Phase diagrams in the absence of an external field

Before we calculate the phase diagrams under the external fields, such as magnetic or electric fields, it is important to

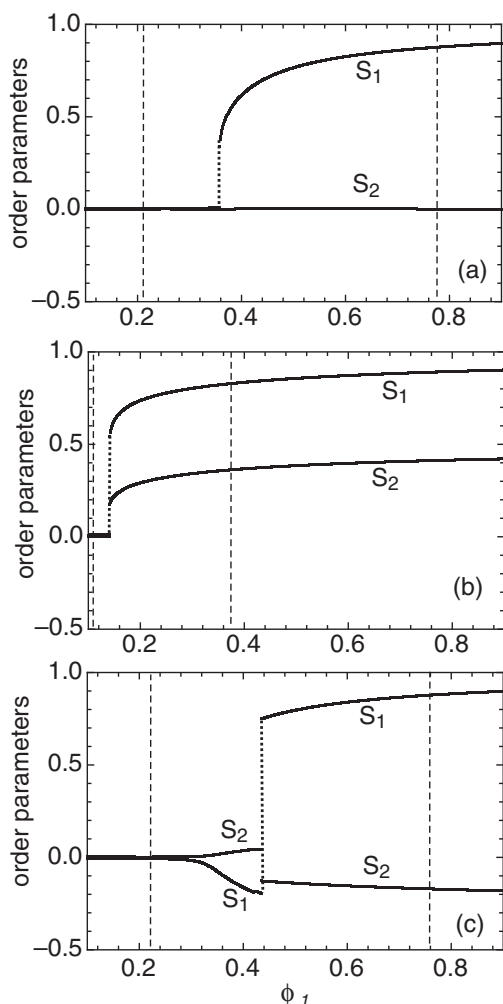


FIG. 3. Order parameters for $c_{12} = 0$ (a), $c_{12} = 0.5$ (b), and $c_{12} = -0.3$ (c) at $\tau = 1.05$ without the external field: $h_1 = h_2 = 0$. The two vertical broken lines denote the isotropic (I) and nematic binodals in Fig. 2.

show the typical phase diagrams in the absence of an external field. We here show three typical phase diagrams. Refer to the previous paper¹⁵ for details.

Figure 2 shows the phase diagrams for $c_{12} = 0$ (a), $c_{12} = 0.5$ (b), and $c_{12} = -0.3$ (c) in the absence of the external field: $h_1 = h_2 = 0$. The solid curve shows the binodal. The dotted line shows the first-order NIT and the dashed line shows the second-order NIT. Figure 3 shows the order parameters for $c_{12} = 0$ (a), $c_{12} = 0.5$ (b), and $c_{12} = -0.3$ (c) at $\tau = 1.05$ in Fig. 2. As shown in Fig. 3(a), in the N^+ phase, the rods are oriented and the LCs are randomly distributed with $S_2 = 0$. At the N_0 phase [Fig. 3(b)], both the rods and LCs are in a nematic phase. In Fig. 3(c), the isotropic phase is continuously changed to the N_1 phase at $\phi_1 \approx 0.31$. Further increasing concentration, we have the first-order N_1 - N_2 phase transition at $\phi_1 \approx 0.42$.

B. Phase diagrams in the presence of an external field

In this subsection, we show some numerical results of the phase diagrams under an external field. Figures 2(a)–2(c) are drastically changed by the external field. Depending on the

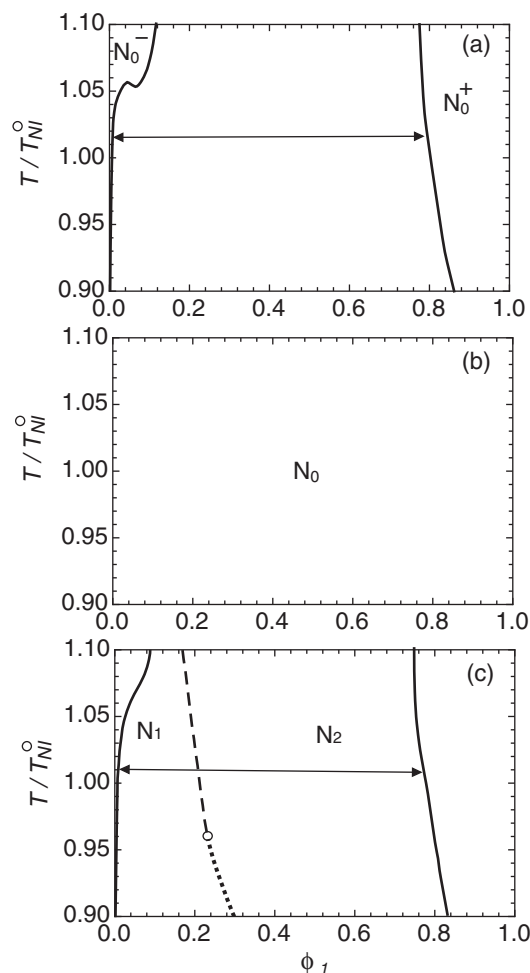


FIG. 4. Phase diagrams for $c_{12} = 0$ (a), $c_{12} = 0.5$ (b), and $c_{12} = -0.3$ (c) with the weak external field: $h_1 = h_2 = 0.1$.

sign of the dielectric anisotropy $\Delta\epsilon_i$ ($i = 1, 2$), we have the following four cases as discussed in Fig. 1.

1. When $\Delta\epsilon_1 > 0$ and $\Delta\epsilon_2 > 0$

Figure 4 shows the phase diagrams under the weak external field: $h_1 = h_2 = 0.1$. When $\Delta\epsilon_1 > 0$ and $\Delta\epsilon_2 > 0$, the rods and LCs favor to align parallel to the direction of the external field and we have $S_1 > 0$ and $S_2 > 0$: N_0 phase, under a strong external field. When $c_{12} = 0$ (Fig. 4(a)), the isotropic phase appeared in Fig. 2(a) disappears and we have two phase coexistence ($N_0^- + N_0^+$) between two paranematic N_0 phases with different concentrations. When $c_{12} = 0.5$ with the attractive interaction between a rod and a LC (Fig. 4(b)), the phase separation $I + N_0$ disappears and we have the stable paranematic N_0 phase. For $c_{12} = -0.3$ (Fig. 4(c)), we have the paranematic N_1 phase at low concentrations, where most LCs align parallel to the direction of the external field and rods are perpendicular to the LCs due to the repulsive interaction $c_{12}(<0)$. On increasing the concentration of rods, the excluded volume between rods prevails the system and the paranematic N_2 phase appears. The isotropic phase appeared in Fig. 2(c) disappears due to the external field and

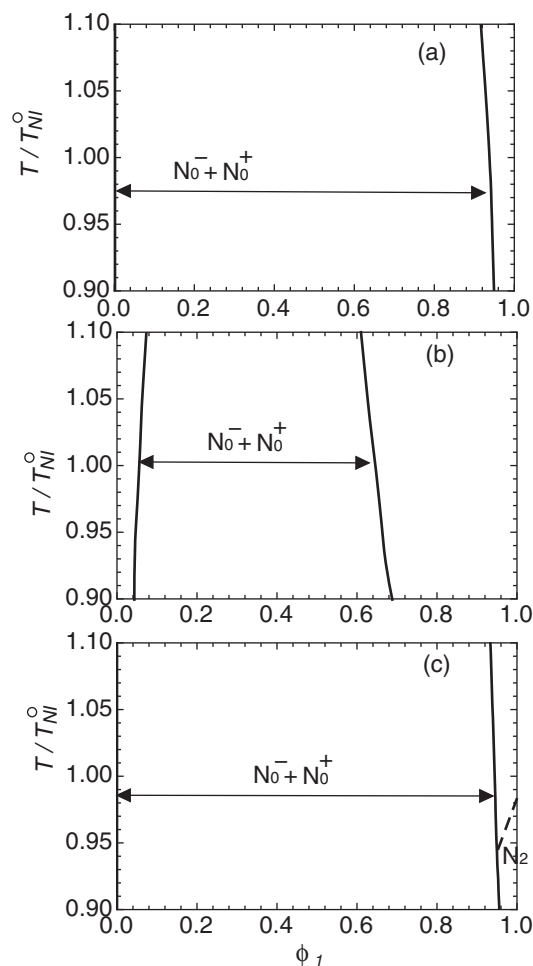


FIG. 5. Phase diagrams for $c_{12} = 0$ (a), $c_{12} = 0.5$ (b), and $c_{12} = -0.3$ (c) with the strong external field: $h_1 = h_2 = 1$.

the N_1 and N_2 phases become stable under the weak external field, where the intermolecular interaction c_{12} prevails the system.

On increasing the strength of the external field h_i , the N_1 and N_2 phases disappear and we have the $N_0^- + N_0^+$ phase separation under the strong external field $h_1 = 1.0$ (see Fig. 5). The stable N_0 phase under a weak external field in Fig. 4(b) is separated into two N_0 phases (Fig. 5(b)). We find that the strong external field induces the phase separations between a rod-rich N_0^+ phase and a rod-poor N_0^- phase.

2. When $\Delta\epsilon_1 < 0$ and $\Delta\epsilon_2 > 0$

Figure 6 shows the phase diagrams under the weak external field: $h_1 = -0.1$ and $h_2 = 0.1$. When $\Delta\epsilon_1 < 0$ and $\Delta\epsilon_2 > 0$, the rods (LCs) favor to align perpendicular (parallel) to the direction of the external field and we have $S_1 < 0$ and $S_2 > 0$: N_1 phase, under a strong external field. When $c_{12} = 0$ (Fig. 6(a)), the isotropic phase disappears and we have the first-order N_1 - N_0 phase transition. In the paranematic N_1 phase at low concentrations, the rods with the negative anisotropy ($\Delta\epsilon_1 < 0$) are randomly distributed on the plane perpendicular to the external field and the LCs with the positive anisotropy ($\Delta\epsilon_2 > 0$) align parallel to the external field.

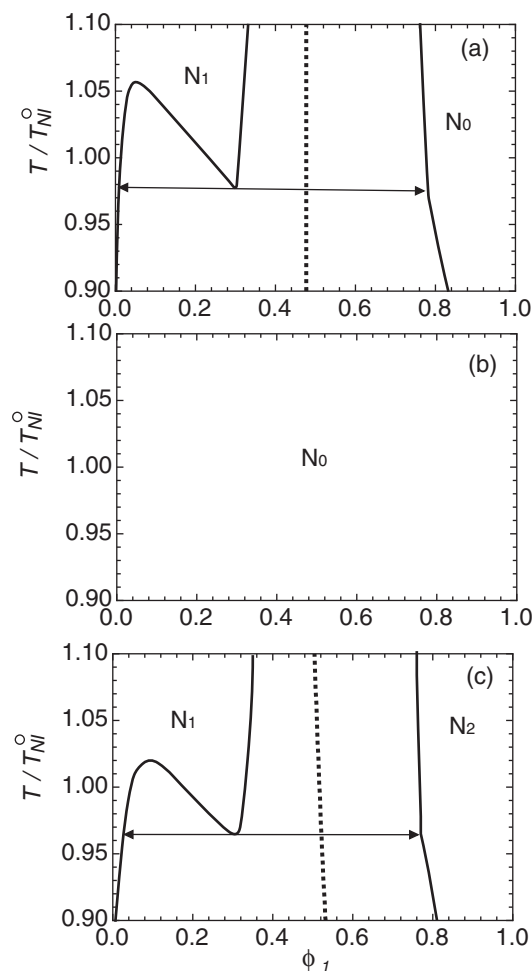


FIG. 6. Phase diagrams for $c_{12} = 0$ (a), $c_{12} = 0.5$ (b), and $c_{12} = -0.3$ (c) with the weak external field: $h_1 = -0.1$ and $h_2 = 0.1$.

On increasing the concentration of rods, the excluded volume interactions between rods prevail the mixtures and we have the N_0 phase. We also have the triple point ($N_1^- + N_1^+ + N_0$) at $\tau \simeq 0.97$. Above the triple point, we have the phase separations: $N_1 + N_0$ and $N_1^- + N_1^+$. When $c_{12} = 0.5$ (Fig. 6(b)), the isotropic phase appeared in Fig. 2(b) shifts to higher temperatures due to the external field and we have the stable paranematic N_0 phase. When $c_{12} = -0.3$ (Fig. 6(c)), the I- N_1 phase transition appeared in Fig. 2(c) disappears and we have the N_1 - N_2 phase transition. On increasing the concentration of rods, the excluded volume interactions between rods prevail the system and the rods align parallel to the direction of the external field and the LCs align perpendicular to the rods because of the repulsive interaction $c_{12} < 0$. We then have the paranematic N_2 phase at high concentrations. We also have the triple point ($N_1^- + N_1^+ + N_2$) at $\tau \simeq 0.96$. On increasing the strength of the external field h_i , the N_0 and N_2 phases in Fig. 6 change to the N_1 phase and we have the $N_1^- + N_1^+$ phase separation, as shown in Fig. 5.

3. When $\Delta\epsilon_1 > 0$ and $\Delta\epsilon_2 < 0$

Figure 7 shows the phase diagrams under the weak external field: $h_1 = 0.1$ and $h_2 = -0.1$, for $\Delta\epsilon_1 > 0$ and $\Delta\epsilon_2 < 0$. In

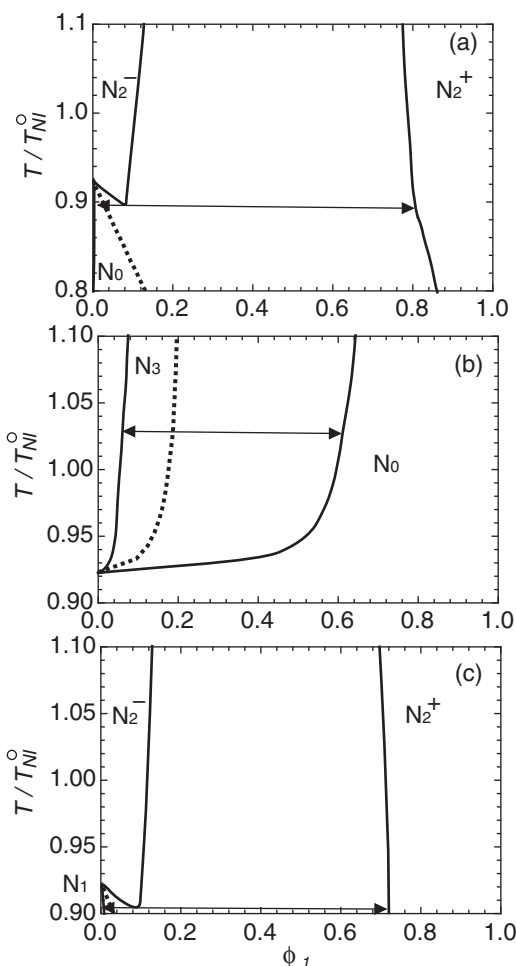


FIG. 7. Phase diagrams for $c_{12} = 0$ (a), $c_{12} = 0.5$ (b), and $c_{12} = -0.3$ (c) with the external field: $h_1 = 0.1$ and $h_2 = -0.1$.

this case, the rods (LCs) favor to align parallel (perpendicular) to the direction of the external field and we have $S_1 > 0$ and $S_2 < 0$: N_2 phase, under a strong external field. When $c_{12} = 0$ (Fig. 7(a)), the isotropic phase disappears and we have the first-order N_0 - N_2 phase transition. In the paranematic N_2 phase, the rods which have the positive dielectric anisotropy ($\Delta\epsilon_1 > 0$) align parallel to the external field and the LCs with the negative anisotropy ($\Delta\epsilon_2 < 0$) are randomly distributed on the plane perpendicular to the external field. At low temperatures and low concentrations, however, the attractive interaction between LCs prevails the system and then the paranematic N_0 phase appears. We also have the triple point ($N_0 + N_2^- + N_2^+$) at $\tau \simeq 0.9$. Above the triple point, we have the phase separations: $N_0 + N_2^-$ and $N_2^- + N_2^+$. When $c_{12} = 0.5$ (Fig. 7(b)), the isotropic phase appeared in Fig. 2(b) shifts to higher temperatures due to the external field and the paranematic N_3 phase appears. At low concentrations, the LCs with the negative dielectric anisotropy align perpendicular to the external field and the rods align parallel to the LCs due to the attractive interaction ($c_{12} > 0$) between the rod and LC and then we have the N_3 phase. The external field is not so strong to form the N_2 phase. On increasing the concentration of rods, the excluded volume interaction between rods prevails the system and the stable paranematic N_0 phase appears.

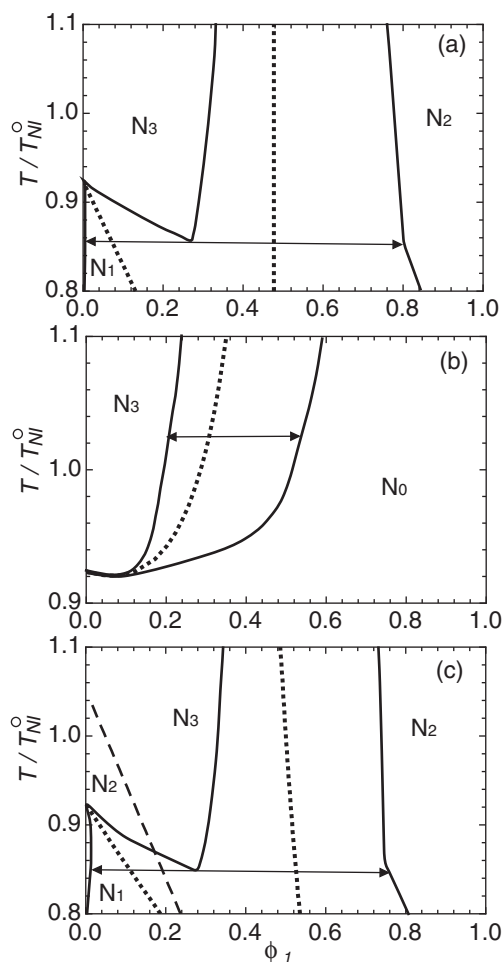


FIG. 8. Phase diagrams for $c_{12} = 0$ (a), $c_{12} = 0.5$ (b), and $c_{12} = -0.3$ (c) with the external field: $h_1 = h_2 = -0.1$.

When $c_{12} = -0.3$ (Fig. 7(c)), the I - N_1 phase transition appeared in Fig. 2(c) disappears and we have the N_1 - N_2 phase transition. We also have the triple point ($N_1^- + N_1^+ + N_2$) at $\tau \simeq 0.91$. On increasing the strength of the external field h_i , the N_0 , N_1 , and N_2 phases in Fig. 7 change to the N_1 phase and we have the $N_1^- + N_1^+$ phase separation under the strong external field.

4. When $\Delta\epsilon_1 < 0$ and $\Delta\epsilon_2 < 0$

Figure 8 shows the phase diagrams under the weak external field: $h_1 = h_2 = -0.1$. When $\Delta\epsilon_1 < 0$ and $\Delta\epsilon_2 < 0$, the rods and LCs favor to align perpendicular to the direction of the external field and we have $S_1 < 0$ and $S_2 < 0$: N_3 phase, under a strong external field. When $c_{12} = 0$ (Fig. 8(a)), the isotropic phase disappears and we have the first-order N_3 - N_2 , N_1 - N_3 phase transitions. In the paranematic N_3 phase, the rods and LCs with the negative anisotropy ($\Delta\epsilon_i < 0$) are randomly distributed on the plane perpendicular to the external field. At lower temperatures, however, the attractive interaction between LCs prevails and the LCs align parallel to the external field and the paranematic N_1 phase appears. On increasing the concentration of rods, the excluded volume between rods prevails the system and the rods align

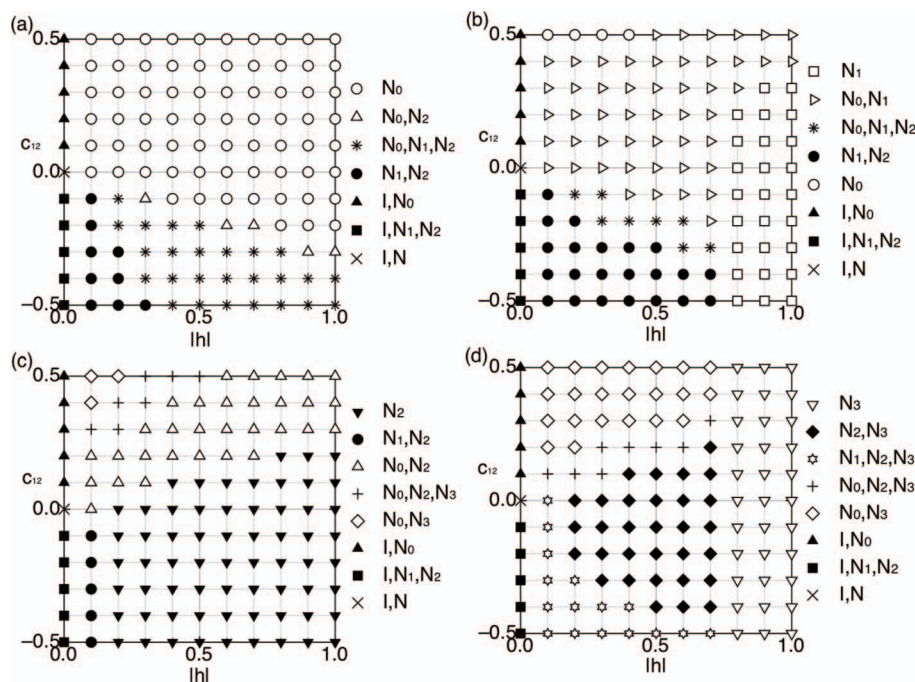


FIG. 9. Possible nematic phases depending on the interaction parameter c_{12} and the external field $|h|$ for $\Delta\epsilon_1 > 0$, $\Delta\epsilon_2 > 0$ (a), $\Delta\epsilon_1 < 0$, $\Delta\epsilon_2 > 0$ (b), $\Delta\epsilon_1 > 0$, $\Delta\epsilon_2 < 0$ (c), and $\Delta\epsilon_1 < 0$, $\Delta\epsilon_2 < 0$ (d). We here take $|h| \equiv |h_1| = |h_2|$. Symbols show the possible nematic phases on the $(|h|, c_{12})$ plane. For example, the symbol \bullet shows that the N_1 or N_2 phase appears on the temperature-concentration plane. Figure 4(c) corresponds to the point $(|h| = 0.1, c_{12} = -0.3)$ in Fig. 9(a).

parallel to the external field. We then have the paranematic N_2 phase. We also have the triple point ($N_1 + N_3 + N_2$) at $\tau \simeq 0.86$. Above the triple point, we have the phase separations: $N_1 + N_3$ and $N_3 + N_2$. When $c_{12} = 0.5$ (Fig. 8(b)), the isotropic phase appeared in Fig. 2(b) shifts to higher temperatures due to the external field and the paranematic N_3 phase appears. On increasing the concentration of rods, the excluded volume interaction between rods prevails the system and the paranematic N_0 phase appears. When $c_{12} = -0.3$ (Fig. 8(c)), the $I-N_1$ phase transition appeared in Fig. 2(c) disappears and we have the first-order N_1-N_2 , N_3-N_2 , and the second-order N_2-N_3 phase transitions. We also have the triple point ($N_1 + N_3 + N_2$) at $\tau \simeq 0.85$. On increasing the strength of the external field h_i , the N_0 , N_1 , and N_2 phases in Fig. 8 changes to the N_1 phase and we have the $N_3^- + N_3^+$ phase separation in the presence of the strong external field.

C. Possible nematic phases

As shown in Subsections III A and III B, the interaction parameter c_{12} and the strength of the external field are important to understand the phase behavior. Figure 9 shows the possible nematic phases on $(|h|, c_{12})$ plane for $\Delta\epsilon_1 > 0$, $\Delta\epsilon_2 > 0$ (a), $\Delta\epsilon_1 < 0$, $\Delta\epsilon_2 > 0$ (b), $\Delta\epsilon_1 > 0$, $\Delta\epsilon_2 < 0$ (c), and $\Delta\epsilon_1 < 0$, $\Delta\epsilon_2 < 0$ (d). We here take $|h| \equiv |h_1| = |h_2|$. Symbols on Fig. 9 show the possible nematic phases on the $(|h|, c_{12})$ plane. For example, the symbol \bullet at $(|h| = 0.1, c_{12} = -0.3)$ in Fig. 9(a) means that the N_1 and N_2 phases, as shown in Fig. 4(c), appear on the temperature-concentration plane. The symbol \circ at $(0.1, 0.5)$ in Fig. 9(b) means that the N_0 phase appears as shown in Fig. 6(b). Figures 4(a)–4(c) correspond to the point $(0.1, 0.0)$, $(0.1, 0.5)$, and $(0.1, -0.3)$ on Fig. 9(a),

respectively. Figures 5(a)–5(c) correspond to the point $(1.0, 0.0)$, $(1.0, 0.5)$, and $(1.0, -0.3)$ on Fig. 9(a), respectively. Figures 6(a)–6(c) correspond to the point $(0.1, 0.0)$, $(0.1, 0.5)$, and $(0.1, -0.3)$ on Fig. 9(b), respectively. Figures 7(a)–7(c) correspond to the point $(0.1, 0.0)$, $(0.1, 0.5)$, and $(0.1, -0.3)$ on Fig. 9(c), respectively. Figures 8(a)–8(c) correspond to the point $(0.1, 0.0)$, $(0.1, 0.5)$, and $(0.1, -0.3)$ on Fig. 9(d), respectively. When $\Delta\epsilon_2 > 0$ (Figs. 9(a) and 9(b)), the N_0 or N_1 phase appears for $c_{12} > 0$ in the weak external field. On increasing the external field, the field prevails the system and we have the N_0 phase for $\Delta\epsilon_1 > 0$, $\Delta\epsilon_2 > 0$ (a) and the N_1 phase for $\Delta\epsilon_1 < 0$, $\Delta\epsilon_2 > 0$ (b). When $\Delta\epsilon_2 < 0$ (Figs. 9(c) and 9(d)), the N_0 , N_2 , or N_3 phase appears for $c_{12} > 0$ in the weak external field. On increasing the external field, the field prevails the system and we have the N_2 phase for $\Delta\epsilon_1 > 0$, $\Delta\epsilon_2 < 0$ (c) and the N_3 phase for $\Delta\epsilon_1 < 0$, $\Delta\epsilon_2 < 0$ (d). We find various nematic phases depending on the strength of the external field and the interaction c_{12} .

IV. SUMMARY

We have theoretically studied the phase diagrams of rod/LC mixtures under an external field. By taking into account two orientational order parameters of the rod and LC, we predict four possible nematic phases (N_0 , N_1 , N_2 , N_3) on the temperature-concentration plane. Depending on the sign of the dielectric (or diamagnetic) anisotropy $\Delta\epsilon_i$ of the rod ($i = 1$) and LC ($i = 2$), we examine the phase behavior for rod/LC mixtures. For example, when the dielectric or diamagnetic anisotropy of rods is positive ($\Delta\epsilon_1 > 0$) and that of LCs is negative ($\Delta\epsilon_2 < 0$), the phase behavior is summarized in Fig. 9(c) on the $(|h|, c_{12})$ plane. In the weak external

field, the interaction between molecules prevails the system and we have the variety phase behavior including N_0 , N_1 , N_2 , and N_3 , depending on the sign of the anisotropy $\Delta\epsilon_i$. In the strong external field, the effect of the external field enhances the phase separations and we have the broad $N_0^- + N_0^+$ phase separations for $\Delta\epsilon_1 > 0$, $\Delta\epsilon_2 > 0$, $N_1^- + N_1^+$ for $\Delta\epsilon_1 < 0$, $\Delta\epsilon_2 > 0$, $N_2^- + N_2^+$ for $\Delta\epsilon_1 > 0$, $\Delta\epsilon_2 < 0$, and $N_3^- + N_3^+$ for $\Delta\epsilon_1 < 0$, $\Delta\epsilon_2 < 0$. We hope our results encourage further experimental and theoretical studies of phase separations of dispersions of rods (nanotubes) in nematic LCs. These results can be useful to obtain the desired director orientation during the phase separation process and new materials with orientational order in rod/LC mixtures.

ACKNOWLEDGMENTS

This work was supported by Grant-in Aid for Scientific Research (C) (Grant No. 23540477) from the Ministry of Education, Culture, Sports, Science and Technology of Japan.

- ¹M. D. Lynch and D. L. Patrick, *Nano Lett.* **2**, 1197 (2002).
- ²I. Dierking, G. Scalia, and P. Morales, *J. Appl. Phys.* **97**, 044309 (2005).
- ³J. M. Russell, S. Oh, I. Larue, O. Zhou, and E. T. Samulski, *Thin Solid Films* **509**, 53 (2006).
- ⁴R. Basu and G. S. Iannacchione, *Appl. Phys. Lett.* **93**, 183105 (2008).
- ⁵R. Basu and G. S. Iannacchione, *J. Appl. Phys.* **106**, 124312 (2009).
- ⁶V. Jayalakshmi and S. K. Prasad, *Appl. Phys. Lett.* **94**, 202106 (2009).
- ⁷S. Courty, J. Mine, A. R. Tajbakhsh, and E. M. Terentjev, *Europhys. Lett.* **64**, 654 (2003).
- ⁸V. Weiss, R. Thiruvengadathan, and O. Regev, *Langmuir* **22**, 854 (2006).
- ⁹J. P. F. Lagerwall, G. Scalia, M. Haluska, U. Dettlaff-Weglikowska, S. Roth, and F. Giesselmann, *Adv. Mater.* **19**, 359 (2007).
- ¹⁰S. Schymura, E. Enz, S. Roth, G. Scalia, and J. P. F. Lagerwall, *Synth. Met.* **159**, 2177 (2009).
- ¹¹H. S. Jeong, Y. K. Ko, Y. H. Kim, D. K. Yoon, and T. T. Jung, *Carbon* **48**, 774 (2010).
- ¹²H. Duran, B. Gazdecki, A. Yamashita, and T. Kyu, *Liq. Cryst.* **32**, 815 (2005).
- ¹³P. van der Schoot, V. Popa-Nita, and S. Kralj, *J. Phys. Chem. B* **112**, 4512 (2008).
- ¹⁴V. Popa-Nita and S. Kralj, *J. Chem. Phys.* **132**, 024902 (2010).
- ¹⁵A. Matsuyama, *J. Chem. Phys.* **132**, 214902 (2010).
- ¹⁶S. Iijima, *Nature (London)* **354**, 56 (1991).
- ¹⁷W. Song, I. A. Kinloch, and A. H. Windle, *Science* **302**, 1 (2003).
- ¹⁸S. Zhang, I. A. Kinloch, and A. H. Windle, *Nano Lett.* **6**, 568 (2006).
- ¹⁹H. G. Chae and S. Kumar, *J. Appl. Polym. Sci.* **100**, 791 (2006).
- ²⁰S. Fraden, G. Maret, D. L. D. Caspar, and R. B. Meyer, *Phys. Rev. Lett.* **63**, 2068 (1989).
- ²¹A. Matsuyama, *Liq. Cryst.* **38**, 729 (2011).
- ²²P. G. de Gennes and J. Prost, *The Physics of Liquid Crystals*, 2nd ed. (Oxford Scientific, London, 1993).
- ²³P. J. Wojtowicz and P. Sheng, *Phys. Lett. A* **48**, 235 (1974).
- ²⁴P. Sheng, *Phys. Rev. Lett.* **37**, 1059 (1976).
- ²⁵S. V. Vasilenko, A. R. Khokholov, and V. P. Shibaev, *Macromolecules* **17**, 2275 (1984).
- ²⁶Z. Lin, H. Zhang, and Y. Yang, *Phys. Rev. E* **58**, 5867 (1998).
- ²⁷A. Matsuyama and K. Kushibe, *J. Chem. Phys.* **132**, 104903 (2010).
- ²⁸P. J. Flory, *Proc. R. Soc. London, Ser. A* **234**, 60 (1956).
- ²⁹L. Onsager, *Ann. N.Y. Acad. Sci.* **51**, 627 (1949).
- ³⁰W. Maier and A. Saupe, *Z. Naturforsch.* **14a**, 882 (1959).
- ³¹F. Brochard, J. Jouffroy, and P. Levinson, *J. Phys.* **45**, 1125 (1984).
- ³²A. Matsuyama and T. Kato, *J. Chem. Phys.* **105**, 1654 (1996).
- ³³A. Matsuyama, *J. Chem. Phys.* **127**, 084906 (2007).
- ³⁴A. Matsuyama and T. Kato, *J. Chem. Phys.* **114**, 3817 (2001).
- ³⁵A. Matsuyama and T. Kato, *J. Chem. Phys.* **108**, 2067 (1998).
- ³⁶S. Zhang and S. Kumar, *Small* **4**, 1270 (2008).
- ³⁷S. Badaire, C. Zakri, M. Maugey, A. Derre, J. N. Barisci, G. Wallace, and P. Poulin, *Adv. Mater.* **17**, 1673 (2005).